# Conference Proceedings of the Society for Experimental Mechanics Series

*Series Editor*

Kristin B. Zimmerman Ph.D.
Society for Experimental Mechanics, Inc.
Bethel, CT, USA

More information about this series at http://www.springer.com/series/8922

Alex Arzoumanidis • Meredith Silberstein • Alireza Amirkhizi
Editors

# Challenges in Mechanics of Time Dependent Materials, Volume 2

## Proceedings of the 2017 Annual Conference on Experimental and Applied Mechanics

Springer

*Editors*
Alex Arzoumanidis
Psylotech, Inc
Evanston, IL, USA

Meredith Silberstein
Department of Mechanical and Aerospace Engineering
Cornell University
Ithaca, NY, USA

Alireza Amirkhizi
UMass Lowell North Campus, Perry 332
University of Massachusetts
Lowell, MA, USA

ISSN 2191-5644 ISSN 2191-5652 (electronic)
Conference Proceedings of the Society for Experimental Mechanics Series
ISBN 978-3-319-63392-3 ISBN 978-3-319-63393-0 (eBook)
DOI 10.1007/978-3-319-63393-0

Library of Congress Control Number: 2015952466

© The Society for Experimental Mechanics, Inc. 2018
This work is subject to copyright. All rights are reserved by the Publisher, whether the whole or part of the material is concerned, specifically the rights of translation, reprinting, reuse of illustrations, recitation, broadcasting, reproduction on microfilms or in any other physical way, and transmission or information storage and retrieval, electronic adaptation, computer software, or by similar or dissimilar methodology now known or hereafter developed.
The use of general descriptive names, registered names, trademarks, service marks, etc. in this publication does not imply, even in the absence of a specific statement, that such names are exempt from the relevant protective laws and regulations and therefore free for general use.
The publisher, the authors and the editors are safe to assume that the advice and information in this book are believed to be true and accurate at the date of publication. Neither the publisher nor the authors or the editors give a warranty, express or implied, with respect to the material contained herein or for any errors or omissions that may have been made. The publisher remains neutral with regard to jurisdictional claims in published maps and institutional affiliations.

Printed on acid-free paper

This Springer imprint is published by Springer Nature
The registered company is Springer International Publishing AG
The registered company address is: Gewerbestrasse 11, 6330 Cham, Switzerland

# Preface

*Challenges in Mechanics of Time-Dependent Materials* represents one of nine volumes of technical papers presented at the SEM 2017 Annual Conference and Exposition on Experimental and Applied Mechanics organized by the Society for Experimental Mechanics and held in Indianapolis, IN, in June 12–15, 2017. The complete proceedings also includes the following volumes: *Dynamic Behavior of Materials; Advancement of Optical Methods in Experimental Mechanics; Mechanics of Biological Systems, Materials and other topics in Experimental and Applied Mechanics; Micro- and Nanomechanics; Mechanics of Composite, Hybrid and Multifunctional Materials; Fracture, Fatigue, Failure and Damage Evolution; Residual Stress, Thermomechanics & Infrared Imaging, Hybrid Techniques and Inverse Problems; and Mechanics of Additive and Advanced Manufacturing*.

Each collection presents early findings from experimental and computational investigations on an important area within experimental mechanics, the mechanics of time-dependent materials being one of these areas.

This track was organized to address constitutive, time (or rate)-dependent constitutive, and fracture/failure behavior of a broad range of materials systems, including prominent research in both experimental and applied mechanics. Papers concentrating on both modeling and experimental aspects of time-dependent materials are included.

The track organizers thank the presenters, authors, and session chairs for their participation and contribution to this track. The support and assistance from the SEM staff is also greatly appreciated.

Evanston, IL, USA — Alex Arzoumanidis
Ithaca, NY, USA — Meredith Silberstein
Lowell, MA, USA — Alireza Amirkhizi

# Contents


1 **Experimental Characterisation of the Mechanical Properties of the Clay-Rock/Concrete Interfaces and Their Evolution in Time** . . . . . 1
Eleni Stavropoulou, Matthieu Briffaut, Frédéric Dufour, and Guillaume Camps

2 **Coupled Anisothermal Chemomechanical Degradation Solutions in One Dimension** . . . . . 5
M. Anguiano, H. Gajendran, R.B. Hall, and A. Masud

3 **Time-Temperature Analysis, DMA and Compression in PBXs** . . . . . 11
Darla Graff Thompson, Jamie Stull, Racci Deluca, and Geoff Brown

4 **Statistical Life Time Prediction Under Tension Loading for Unidirectional CFRP with Thermoplastics as Matrices** . . . . . 19
Masayuki Nakada, Yoko Morisawa, and Yasushi Miyano

5 **Time and Temperature Dependence on Tensile Strength of Unidirectional CFRP with Various Carbon Fibers** . . . . . 25
Yasushi Miyano, Yoshiki Kobayashi, and Masayuki Nakada

6 **Time Temperature Superposition and Prony Series Coefficients of Asphalt Roof Shingle Material from Viscoelastic Creep Testing** . . . . . 33
Sreehari Rajan, Michael A. Sutton, Ryan Fuerte, and Igor Emri

7 **A Mixture Theory with Interactive Body Forces for Composite Interphases** . . . . . 39
R.B. Hall

8 **Material Creep Behavior with Prediction of Tertiary Creep Failure by a Spherical Micro-indentation Method** . . . . . 43
Dumbi C. Otunyo and Bruce S. Kang

9 **Mechanical and Biodegradable Behavior of AZ31 Magnesium Alloy Immersed in Simulated Body Fluid** . . . . . 49
Wenxue Lin, Ning Zou, and Qizhen Z. Li

10 **Failure of Laser Welded Structures Subjected to Multiaxial Loading: Experimental Development** . . . . . 57
Bonnie R. Antoun and Kevin Connelly

11 **Characterization and Modeling of PEEK in Histories with Reverse Loading** . . . . . 65
Wenlong Li, George Gazonas, Eric N. Brown, Philip J. Rae, and Mehrdad Negahban

12 **A Biomimetic Composite for Space Vehicle/Habitat Design** . . . . . 71
Ashok Kumar Ghosh, Ramon Martinez, and Carl M. Cady

**13 Molecular Dynamics Motivated Maxwell Element Spring Nonlinearity** . . . . . 79
G.A. Arzoumanidis, T.J.L. Mustard, M.D. Halls, and Stephen Christensen

**14 Characterization and Simulation of Time-Dependent Response of Structural Materials for Aero Structures and Turbine Engines** . . . . . 83
Stephan M. Russ, Reji John, and Craig P. Przybyla

**Topic: A Biomimetic Composite for Space Vehicle/Habitat Design**

**By**

**Ashok Kumar Ghosh [(1)], Ramon Martinez [(1)] and Carl M. Cady [(2)]**
1- Mechanical Engineering Department, New Mexico Tech
2- Material Science in Radiation and Dynamic Extremes, Los Alamos National Lab.

**Abstract:**

There are plenty of literature dealing with studies that demonstrate how Noise and Vibration can interfere with space crew's ability to perform critical mission functions especially at the time of launch, launch abort, and reentry. Space habitat like the ISS functions as spaceflight crew's home; their workshop; office; and laboratory. All these activities result in a complex noise/vibration environment. This paper discusses the stiffness characteristics of a time dependent composite that has a soft middle porous layer, infused with a compatible fluid and is covered with thin sheets of skin layers on both the faces. Tests demonstrated that this design could lead to improvement in product performance, designed for acoustics /vibration isolation environment. The design has the flexibility to adapt its characteristics to suit various end application environments.

## 1.0 Introduction

Space Habitat like the ISS functions as spaceflight crew's home; their workshop; office; and laboratory. All these activities generate a complex noise/vibration environment that has two distinct characteristics: a) continuous (from pumps, fans, compressors, avionics, and others), and b) intermittent (from exercise equipment, carbon-di-oxide removal system, etc.). [1]

In nature, shape and structure evolve from the struggle for better performance. Human "Skull Structure" encloses/protects our brain, performs similar function as that by space Vehicle/Habitat structure. Proposed composite is a Fluid Filled Cellular Composite (FFCC) Structure that has a soft middle open-cell porous layer, which can be infused with a compatible fluid like water and is covered with thin sheets on both the faces. Extensive tests demonstrated that the FFCC design can lead to dramatic improvement in products, designed for acoustics/vibration isolation; impact & explosive resistance; radiation shielding; and thermal management characteristics. Above all, the FFCC design has the flexibility to adapt its characteristics to suit end application environment.

Dawson et al. [2-4] developed an improved relation between the permeability, porosity and compressive strain of open-cell foams filled with Newtonian and non-Newtonian liquid subjected to compressive strains. Fluid flow through an open-cell foam usually contributes to the elastic moduli if the fluid has a high viscosity or if the strain-rate is exceptionally high, Tyler et al. [5]. Cell fluids contribute to the strength of open cell foams in a completely different way. Ghosh et al [6] have demonstrated that it is possible to engineer FFCC to attenuate vibration in a wide frequency range. Chalasani [7] compared the ride performance limits of active and passive suspensions using a quarter car model.

## 1.1 Idealization

The FFCC has a sandwiched construction with skin layers (Kevlar) at both the faces together with a core layer of open-cell, quick-recovery, super-resilient polyurethane foam material with interstitial pores filled with a compatible fluid. Cells in the core layer have wide variation in shape and size. The unique morphology of this core layer will make the FFCC valuable for various end applications.

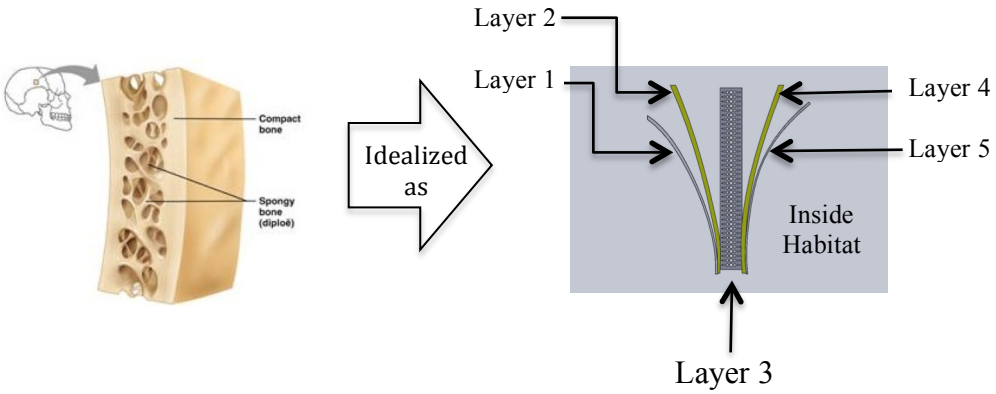


Figure 1: (left) Human Skull showing compact and cancellous bones (right) Idealized Skull wall section showing core and exterior/interior skin layers.

Description on these layers is given below:

I. Layer 1 (Exterior) – A thin flexible film that will protect the inner layers from UV radiation.
II. Layer 2 (Outer skin layer) - A fiber reinforced plastic layer/s made from fabric of high strength long fiber such as Kevlar, fiberglass, carbon fiber, ballistic nylon or Nomex. Selection of the right material was determined using a Quality Function Deployment (QFD) analysis. Once the materials are selected, their characterization took place following ASTM D 3039 & D3515 specifications to determine the anisotropic elastic constants $E_1$, E2, $\mu_{12}$ , $\mu_{21}$ and $G_{12}$ values.
III. Layer 3 (Core layer) – A cellular structure that has morphology similar to skull's cancellous structure. A quick recovery open-cell polyurethane (PUF) with stress-strain behavior similar to Cancellous bone is used.
IV. Layer 4 (Inner skin layer) – This layer can be same as layer 2 or different. Selection will be done using QFD analysis.
V. Layer 5 (Innermost layer) – Similar to layer 1 but the material for this layer will be selected to provide thermal and visual comfort to the astronauts. It may be a stress-sensitive layer that will indicate over-stress in the system.

Current investigation deals with core layer.

## 1.2 Core Layer

PORON® microcellular urethane foam is a product manufactured by Rogers Corporation that was developed in 1980s for industrial and electronics applications. It is a fine pitch open cell

urethane foam with average cell size is approximately 100 microns. Typical compressive strength at 25% deflection based on test done at a compression rate of 0.2 inch/min (i.e. 0.085 mm/sec) is 21kPa (refer to column 3 of the data sheet). Corresponding values for soft and firm foams are 41 kPa, and 69 kPa respectively.

### 1.3 Cell Morphology

Using Scanning Electron Microscopy (SEM), this study analyzes the morphology of the cells that form the porous structure. SEM analysis was performed at the Material Engineering Department at New Mexico Tech using Hitachi S-4100 Field Emission SEM. Figure 2 has the SEM pictures of cells cut by the cutting plane for very soft (VS) and Soft (S) foams used in this study. Cell size distribution parameters for VS and S are given in the boxes below each picture. Total number, #, of cells in a given area is inversely proportional to the stiffness of the overall foam structure. Lesser number of cells means larger wall thickness of the cells and higher stiffness. Cells near the upper and lower surfaces are smaller than the ones at the middle due to mold wall effects during the foaming process. Densities for VS, S and F foams measured as 235 kg/m$^3$, 245 kg/m$^3$ and 265 kg/m$^3$ respectively.

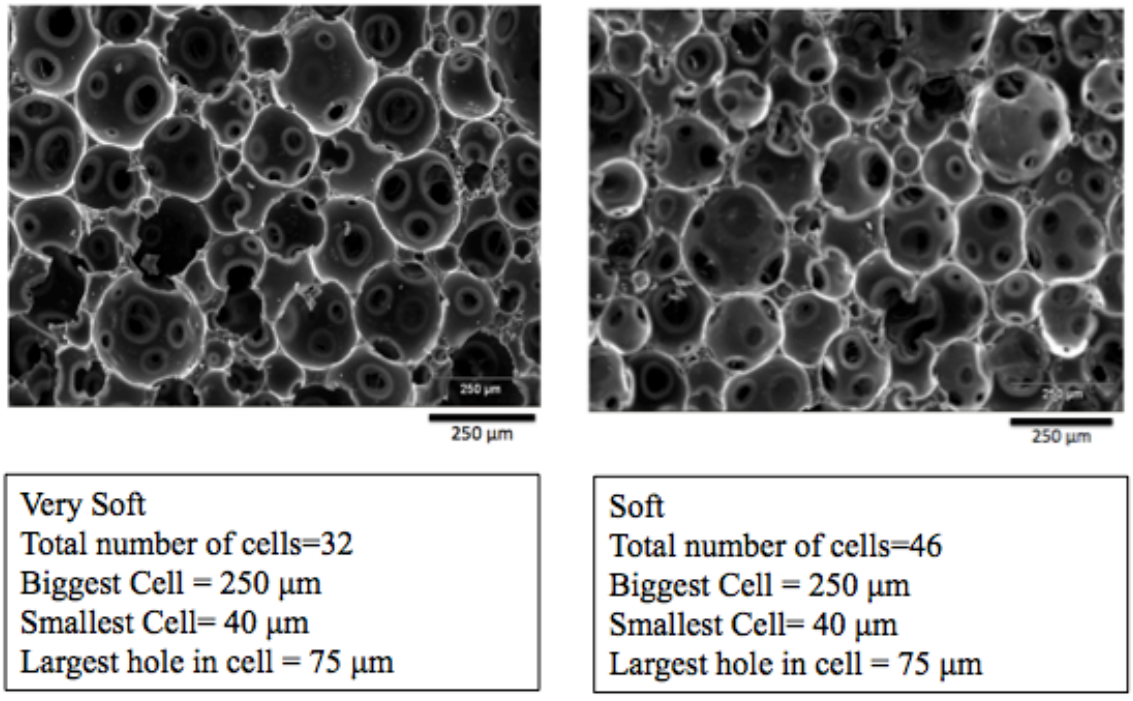


Figure 2: PU Foam Cell Size distribution as seen under SEM

Magnified view of a typical cell is given in figure 3 (left). Cell size distribution in a quantitative scale is plotted and given in figure 3(right). In the same area, there were 32 and 46 cells for very soft and soft foam respectively. Average diameters of cells for soft and very soft foam are 132µm and 172µm respectively. Largest interconnected hole diameter was found to be around 75µm for both the foams. The transport properties of the foams will depend on both cell size distribution and diameter of the interconnected holes.

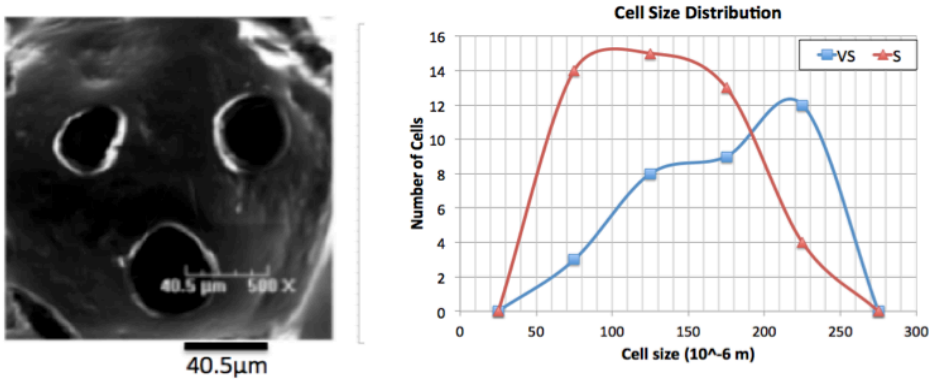


Figure 3: (left) Magnified view of a single cell of the foam (magnification 500) [6]; (right) Cell size distribution

## 2.0 PU Foam Mechanics

The engineering stress-strain behavior of typical PU foam under compression is given in figure 4. $\varepsilon_d$ is the densification strain (DS), the value of which will vary with the softness of the foam. The DS values are provided in table 1. Conforming to Manufacturer's indicator, authors have used the same indicator to compare different foams. Engineering stress corresponding to compression of 25% obtained from test performed at strain rate of 0.01 $s^{-1}$ will be defined as "compression resistance (CR)" and the same value will be used to validate manufacturer specified data. Table 1 demonstrates the validation of the current test values for all the three foams. Area between the curve and the x-axis in figure 4 represents the amount of energy absorbed per unit volume during the compression process, which is an indicator of toughness of the sample.

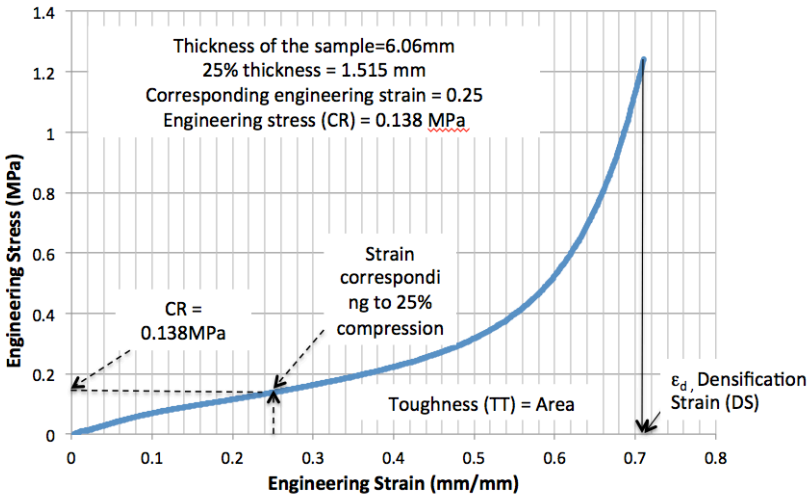


Figure 4: A typical engineering stress-strain loading curve under compression.

## 2.1 Test Setup

Rectangular samples are cut from five different foam plates and tested under compression using MTS 880 universal testing machine. Four different strain rates (0.001, 0.01, 0.1 and 1.0 $s^{-1}$) are investigated. Figure 5 (Top) shows the testing machine with the sample holder supported on the bottom platen of the machine. Sample holder is carefully designed and fabricated so that the same holder can be used for multiple tests. The construction details of the sample holder are given in figure 5 (Bottom). Three plates, top, middle and bottom, will create two closed chambers. Top closed chamber located between the top and middle plates will house the sample. Arrangement is made to pressurize the fluid in the sample. Bottom closed chamber is primarily to create a region where air will be at a different pressure from the ambient pressure. Thus, it is possible to characterize the sample by exposing its two faces at two different pressure environments.

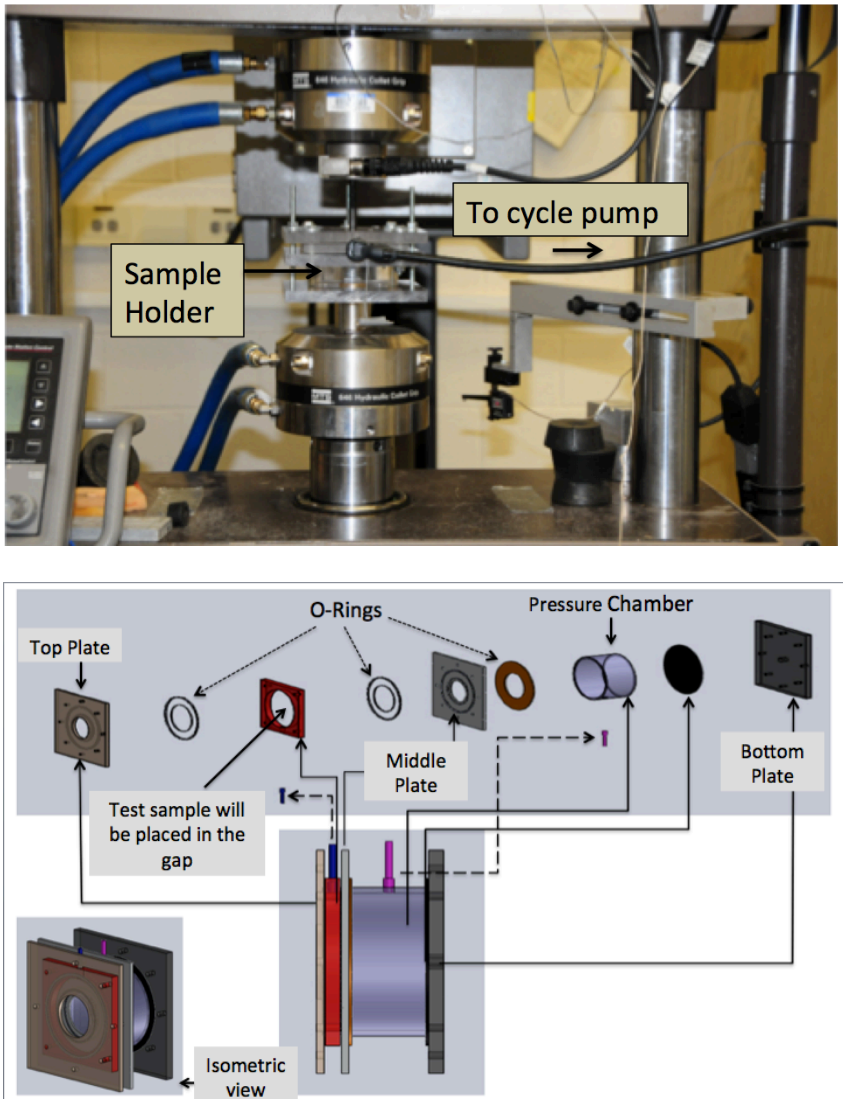


Figure 5: (Top) Sample holder is placed on the bottom platen of the MTS 880 testing machine; (Bottom) Construction details of the sample holder.

An important characteristic of FFCC structure is its attenuation of acoustic energy. When FFCC structures are exposed to acoustic loads, two mechanisms contribute towards absorption of the acoustic energy significantly better than that in a homogenous material: a) losses due to viscous flow through pores, and b) internal friction. Individual contribution of each will depend on parameters like: a) characteristics of the porous structure, b) characteristics of the infused fluid, and c) characteristics of the loads. Low (250 Hz to 1 kHz) frequency acoustic transmission loss (TL) of FFCC is found to be 25% higher than that for a homogenous material having the same mass per unit area.

After 3 cycles of loading and unloading, amount of water that is drawn in the interstitial pores is determined by weighing the samples before and after the tests. From the difference in their weights, and knowing initial volume and density of solid foam, amount of fluid in the interstitial pores is calculated and the same are plotted in figure 6. Both very soft and soft foams were tested under 3-cycles of loading unloading at three different strain rates 0.01, 0.1 and 1.0 sec $^{-1}$ in water medium. Very soft foam is almost insensitive to compression rate whereas the soft foam needs slower rate for higher replacement of air with water at room temperature.

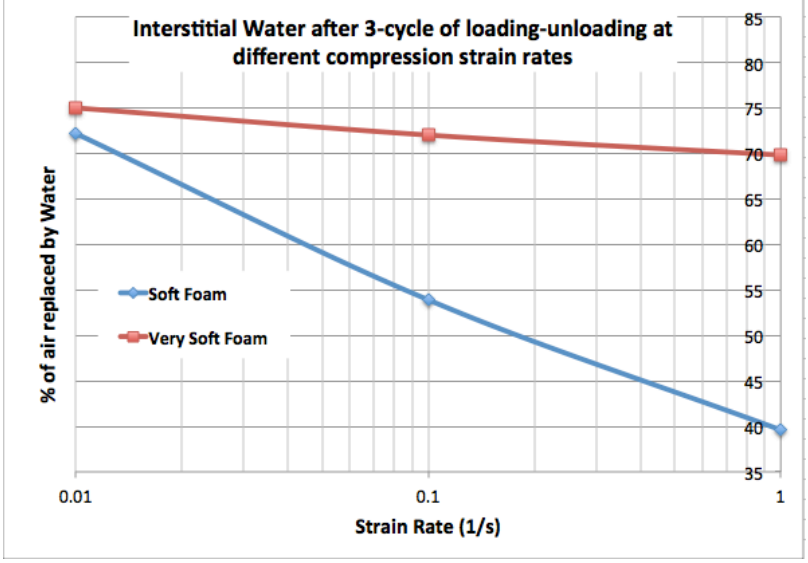


Figure 6: Interstitial water absorption with strain rate and foam type

## 2.6 Observations and discussion

Table 1 gives the mechanical characteristics of firm, soft and very soft foams, and comparison with the manufacturer supplied product data. Column 1 has the sample identification numbers. Column 2 defines the foam type (FT); Sample dimensions (SD) are given in column 3. Column 4 gives the strain rate (SR) used in current test; densification strain (DS), $\varepsilon_d$, is given in column 5; 25% deformation (D) given in column 6; corresponding engineering strain, 25% $\varepsilon$ is given in column 7 and column 8 has compression resistance, CR and the last column has % difference

from Manufacturer's data (MD). Percentage difference in CR values demonstrates that the testing process adopted is acceptable.

Table 1: Validation of experimental values with manufacturer's data

| ID # | FT | SD, (mm) | SR ($s^{-1}$) | DS, $\varepsilon_d$ (m/m) | 25% D, mm | 25% ε | CR, kPa | % diff. MD |
|---|---|---|---|---|---|---|---|---|
| 1 | Very Soft (VS) | 20.85 x 25.77x6.36 | 0.01 | 0.80594 | 1.59 | 0.25023 | 22.05 | +5.0 |
| 2 | Soft (S) | 20.35x26.25x6.45 | 0.01 | 0.70403 | 1.6125 | 0.24989 | 44.09 | +7.5 |
| 3 | Firm (F) | 21.17x26.61x6.18 | 0.01 | 0.73435 | 1.545 | 0.25041 | 85.14 | +23 |

Figure 7 has plots showing how compression resistance (CR) values vary with successive loading cycles. Two strain rates are tabulated with one being 10 times than that of the other. The compression resistance, CR, is highest for cycle 1 and falls for each subsequent cycle. This is due to the Mullin's effect. After 2nd cycle, foams reach steady state and become insensitive to changes in subsequent cycles.

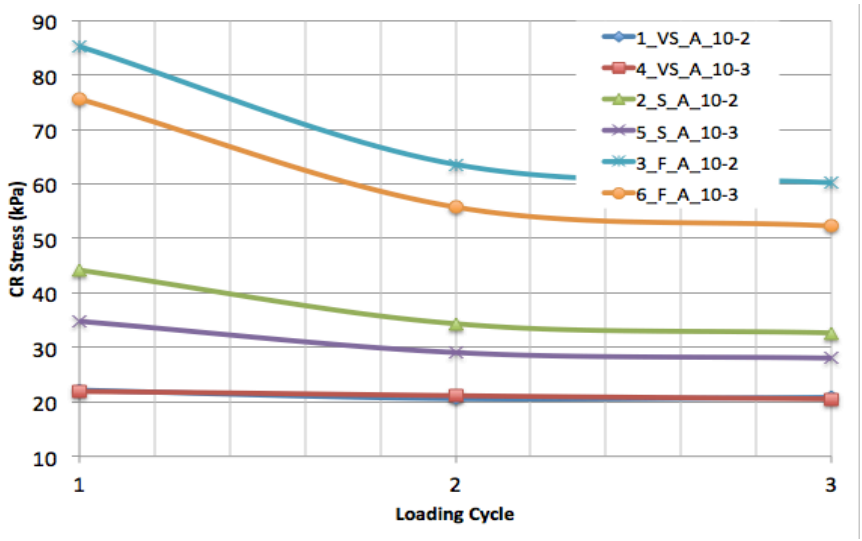


Figure 7: Variation of Compression Resistance with loading cycles and strain rate in air media

## 2.7 Conclusions

Sensitivity of CR values to strain rate decreases with the softness of the foam. Thus, it is easier to compress foam at a slower rate. Typically, polymers show-strengthening effect as a function of increased strain rate. It is likely that the minimal change in strain rates was not large enough to exhibit significant differences in the case of lower density foams but were more apparent in the case of the higher density foams.

3.0 References:


[1] Evidence Report: Risk of Incompatible Vehicle/Habitat Design, HRP, March 08, 2013.

[2] M.A. Dawson, G.H. McKinley, & L.J. Gibson, "The Dynamic Compressive Response of Open-Cell Foam Impregnated With a Newtonian Fluid", J. of Applied Mechanics, July 2008, Vol. 75.

[3] M.A. Dawson, G.H. McKinley, & L.J. Gibson, "The Dynamic Compressive Response of an Open-Cell Foam Impregnated With a Non-Newtonian Fluid", J. of Applied Mechanics, Nov 2009, Vol. 76.

[4] M.A. Dawson, J.T. Germaine, L.J. Gibson, Permeability of open- cell foams under compressive strain. Int. J. of Solids & Structures. 44, 5133–5145 (2007)

[5] Tyler, C. J., and Ashby, M.F., "Project Report, Cambridge University Engineering Department, 1986.

[6] A.K.Ghosh, A.D.Williams, J.M.Zucker, J.L.Mathews and N. Spinhirne, "An Experimental Investigation into the Acoustic Characteristics of Fluid-filled Porous Structures – A Simplified Model of the Human Skull Cancellous Structures", J. of Experimental Mechanics, April 2008.

[7] R. M. Chalasani, "Ride Performance Potentials of Active Suspension System – Part I: Simplified Analysis Based on a Quarter-Car Model," Symposium on Simulation and Control of Ground Vehicles and Transportation Systems, ASME Monograph, AMD, vol. 80, no. 2, pp. 187-204, 1986.